

LM-00K045
July 7, 2000

Interface Reactions and Electrical Characteristics of Au/GaSb Contacts

H. Ehsani, R.J. Gutmann, G.W. Charache

NOTICE

This report was prepared as an account of work sponsored by the United States Government. Neither the United States, nor the United States Department of Energy, nor any of their employees, nor any of their contractors, subcontractors, or their employees, makes any warranty, express or implied, or assumes any legal liability or responsibility for the accuracy, completeness or usefulness of any information, apparatus, product or process disclosed, or represents that its use would not infringe privately owned rights.

I. INTRODUCTION

There is considerable interest in GaSb and GaSb-based alloys because of their potential in numerous opto-electronic and high speed electronic devices¹⁻³, including: thermophotovoltaic (TPV) diodes^{4,5}, high electron mobility and heterojunction bipolar transistors⁶, and IR-laser and waveguides⁷. These devices often impose stringent requirements on metallization technology. Interface reactions, depth of the reactions, and phase transitions upon annealing can have significant influence on the device performance. Understanding of underlying mechanisms makes possible improvement of the resistivity, stability, and reliability of the contacts. Compared to GaAs⁸⁻⁹ and InP¹⁰, relatively little information has been reported about the structural and electrical properties of metal contacts with GaSb and related alloys.

It is well established that in compound semiconductors the surface Fermi-level is pinned after coverage of a sub-monolayer of metal. The degree of Fermi-level pinning in some semiconductors such as GaAs or GaSb¹¹⁻¹² is independent of the type of metal. The Fermi-level pinning in most metal/semiconductor interfaces cause difficulty in forming ohmic contacts. In these semiconductors, the mechanism for ohmic contact formation is not a function of the metal work function. Instead, ohmic contact formation requires a high doping concentration on the semiconductor surface and thus current transport is dominated by tunneling¹³. Photoemission spectroscopy measurements by Spicer et al.¹⁴ revealed that the position of the surface Fermi-level in metal/GaSb contacts is near the valance band. This large pinning of the surface Fermi-level in metal/n-type GaSb often necessitates annealing during ohmic contact formation.

Au and Au-based alloys such as Au-Zn and Au-Ge are widely used¹⁵⁻¹⁶ to make electrical contacts to the p-type and n-type GaSb and GaSb-based alloys. Similar to Au/GaAs¹⁷⁻¹⁹ or Au/InP²⁰⁻²¹ contacts, ohmic contacts to n-type GaSb require annealing²²⁻²³. This process is often accompanied by interdiffusion, interface reactions, and phase transitions that affect reliability, device performance and depth of contacts. For instance, electrical contacts to shallow junction devices require precise control of: reaction depth, interface reactions, interdiffusion, and thermal stability. In particular, Au is found to be extremely reactive with GaSb in comparison with other III-V compound semiconductors. Thus, understanding the mechanism of interface reactions and correlation of the reactions

with electrical behavior of Au/GaSb contacts are of fundamental importance. However, current reports on the Au/GaSb contacts are mostly oriented toward the electrical characteristics of the Au-based alloy contacts, often at relatively high annealing temperatures (>250 °C) and long annealing times^{15-16,24-31} (minutes to hours). No detail investigation of the structural properties and the correlation between the structural and electrical characteristics of the contacts has been reported.

In this paper a systematic study of the structural, chemical, and electrical properties of Au/GaSb contacts are presented. The effect of annealing temperature and time on the reaction kinetics and structural properties of the contacts is emphasized, along with the influence of interface reaction and phase transition on electrical properties. The specific contact resistivity of Au contacts with n-type and p-type GaSb are presented. Finally, a possible mechanism for the transition from a Schottky to ohmic contact is discussed.

II. EXPERIMENTAL PROCEDURES

Single-crystal (001) oriented n-GaSb (Te-doped) wafers with carrier concentrations of $5-8 \times 10^{17} \text{ cm}^{-3}$ and p-GaSb wafers with carrier concentrations of $4-5 \times 10^{17} \text{ cm}^{-3}$ were used for all measurements. Prior to both backside and front-side metallization, all GaSb samples were cleaned by immersing the samples in organic solvents and then in HCl for about 3-5 minutes, followed by etching in diluted HF in DI water (1:20) for 30 seconds and a final de-ionized water rinse. Au films were deposited in an electron beam evaporator with a base pressure of $3-5 \times 10^{-7}$ Torr. Ohmic contacts were first formed on the back-side of the wafer, by evaporating 0.5- μm -thick film of Au and annealing at 300 °C for 30 seconds. Annealing was performed in a rapid thermal annealing (RTA) system in N_2 ambient. Front-side metallization employed circular contacts ranging from 30 μm to 200 μm diameter, using lift-off patterning technique.

The microstructural properties and depth of the Au/GaSb contact as a function of annealing temperature were investigated using cross-sectional scanning electron microscopy (CSSEM) images. For the analyses of the phase formations and phase transitions, x-ray diffraction using $\text{CuK}\alpha$ radiation operated at 40 KV and 30 mA was used. The depth profile of Au and other related elements were characterized using

secondary ion mass spectroscopy (SIMS) measurements. The electrical properties of these samples were studied by measurement the I-V characteristics of the contact on circular contacts with different diameters. Specific contact resistance was obtained using the Cox and Strack technique³².

III. EXPERIMENTAL RESULTS

A. Interaction Kinetics

Gold films, both 0.05- μm and 0.5- μm -thick, were deposited with and without the circular contact pattern. Visual observation demonstrated that the as-deposited gold color of 0.05- μm -thick film changed to a light milky color after annealing at 150 °C for 3 seconds. The gold color of the 0.5- μm -thick film also changed to a light milky color after annealing at 100 °C for about 1.8 hours, at 150 °C for about 5 minutes, and at 200 °C for about 40 seconds. The change of the surface color was very rapid (less than a few seconds) when the samples were annealed at elevated temperatures (> 250 °C). The change in the surface appearance indicated that chemical reaction between the Au film and the GaSb substrate occurred. It is shown later that the entire Au film has reacted with GaSb when the surface color changed. The time of gold color disappearance as a function of the annealing temperature was used to obtain a value of activation energy for the reaction of Au with GaSb. Figure 1 shows an Arrhenius plot of temperature dependence of the reaction time, indicating an activation energy of 0.82 eV. For comparison, we deposited 0.5- μm -thick Au film on (001) GaAs substrates and annealed these samples side by side with the Au/GaSb samples. No change of surface color was observed on Au/GaAs samples, even after annealing at 400 °C for 30 seconds. This result indicates that the reaction of Au with GaAs is slower than with GaSb.

B. Reaction Depth

Figures 2(a)-2(d) represent a sequence of CSSEM images of a 0.5- μm -thick Au film deposited on a (001) GaSb substrate and annealed at different temperatures and times. Figure 2(a) illustrates the as-deposited interface of Au on GaSb, indicating a sharp change in image contrast at the interface. (The bright line at the Au/GaSb interface is attributed to the shadow of the Au apex when the sample was cleaved after the

deposition. Attempt for eliminating the Au apex through polishing has not been pursued mainly because the damage due to polishing effects on the image of the contact). Chye et al.¹² observed the development of a few monolayers of intermixing of Au with GaSb on cleaved (110) GaSb surface at the as-deposited temperature. However, CSSEM images are not capable of determination of a few monolayers intermixing at the interface. Figure 2(b) shows the micrograph of the sample annealed at 150 °C for 5 minutes. Two distinct layers, above and below the original interface are observed. The shape of polycrystalline grains below the original interface (bottom layer) is preferentially elongated perpendicular to the interface, whereas no preferential shape of polycrystalline grains is observed above the original interface (top layer). The thickness of the top layer is smaller than the bottom layer. In addition, the interface between GaSb substrate and the bottom layer remains abrupt. Figure 2(c) shows the micrograph of the sample annealed at 300 °C for 30 seconds. Again two regions can be seen on GaSb surface. Comparison of Figures 2(b) and 2(c) indicates that the size of the polycrystalline grains and the total reaction thickness increased with annealing temperature. The surface morphology of this sample is slightly rough, but no pits or hillocks with preferential orientation are observed which have been reported in Au/GaAs contact samples¹⁹. The difference in size and shape of the polycrystalline grains in the layers above and below the original interface is perhaps an indication that these two layers have a different crystalline structure. Figure 2(d) shows the micrograph of the contact annealed at 400 °C for 30 seconds. In this figure no abrupt interfaces are observed and the surface morphology is rough. Plane view SEM and optical microscopy showed that dark spots are scattered on the surface in addition to the increased surface roughness.

C. Chemical Reactions

X-ray diffraction (XRD) measurements were performed to investigate the effect of annealing temperature on the interface reactions and phase transitions of Au/(001)GaSb contacts. Figure 3 illustrates the XRD spectra of the as-deposited 0.5- μm -thick Au on GaSb, which shows intensity peaks corresponding to polycrystalline gold and single-crystal GaSb. When the sample was annealed at 100 °C for 1.8 hours, the XRD spectra significantly changed and peaks corresponding to AuSb₂ and Au₇Ga_{2+x} alloy

(β phase) were obtained [Fig. 4]. As mentioned above, this annealing time corresponds to the time required for the change of surface color. Since XRD does not detect any peaks corresponding to elemental Au, it appears that the entire Au film reacted with GaSb. The XRD spectra of Figure 4 also shows that the relative intensity of AuSb_2 peaks are stronger in the $\langle 100 \rangle$ orientation in comparison with the relative intensity of standard powder diffraction peaks. This difference indicates that the polycrystalline grains of AuSb_2 are partially ordered with respect to the substrate. Concentration of the Ga atoms in Au at the 100 °C annealing temperature is approximately 20%, which is much larger than the solid solubility of Ga in Au at this temperature (less than 4%). Thus, the concentration of Ga in Au is not controlled by solid solubility. In contrast, the interface reaction of Au with GaAs or GaP takes place at temperatures above 300 °C and the concentration of Ga atoms in Au at the reaction temperature is in the solid-solubility range (approximately 12% at 400 °C). Significant reaction products involving the group V elements were not reported in either the Au-GaP³³ or Au-GaAs¹⁹ systems.

The XRD spectra of a sample annealed at 150 °C for 5 minutes shows appearance of additional peaks corresponding to the Au_2Ga alloy (γ phase)[Fig. 5]. Figure 6 shows the results of a 0.5- μm -thick Au film deposited on (001) GaSb, which was then annealed at 250 °C for 30 seconds. AuSb_2 , AuGa, Au_2Ga , and $\text{Au}_7\text{Ga}_{2+x}$ phases appear in the diffraction pattern. When the sample was annealed at 300 °C for 30 seconds, all the peaks corresponding to the $\text{Au}_7\text{Ga}_{2+x}$ phases vanished and the intensity of AuGa peaks increased, as shown in Fig. 7. With a sample annealed at 300 °C for 20 minutes, the XRD spectrum remains identical to Fig. 7, except that the intensity of AuGa peaks increased and the intensity of the Au_2Ga peaks decreased. Similar results were observed when the sample annealed at 350 °C for 30 seconds. XRD spectra of the sample annealed at 400 °C for 30 seconds showed peaks of GaSb, AuSb_2 , AuGa, Au_2Ga , and AuGa_2 , [Fig. 8].

D. Distribution of the Elements

Secondary Ion Mass Spectroscopy (SIMS) depth profiling was conducted to analyze the distribution and concentration of Au, Ga, Sb, Te (dopant in the substrate), C, and O_2 in the Au-GaSb system. Figure 9(a) shows the SIMS depth profile of Au, Ga, and Sb of a 0.5- μm -thick Au-film deposited on n-type GaSb and annealed at 150 °C for 5

minutes. This figure indicates an abrupt step in the concentration profiles of Au, Sb, and Ga at the original interface (about 0.4 μm below the surface) which is consistent with CSSEM micrograph [Figure 2(b)]. Figure 9(a) shows that the Sb concentration in the layer above the original interface is negligible, indicating that Sb (AuSb_2 phase) is formed in the layer adjacent to GaSb substrate (0.4-1.0 μm). Note that the decrease in relative concentration of Sb in the AuSb_2 layer in comparison with the GaSb substrate is due to different sputtering and/or ionization yields in these two compounds. On the other hand, Ga atoms appeared in both layers, with the concentration of Ga in the layer above the original interface larger than that in the layer below the original interface. The interface of these two layers is also determined by the presence of C and O_2 in this region, as illustrated in Figure 9(b). The C and O_2 remain almost inert, without any significant diffusion into either layer.

Since the original interface does not shift significantly in Fig. 9, we conclude that when Au reacts with Sb on the GaSb surface, a large fraction of the released Ga atoms out-diffuse, forming alloys and/or compounds with Au. Figure 9(b) also shows that the concentration of Te decreases from 10^{18} cm^{-3} in GaSb substrate to mid 10^{16} cm^{-3} in the layer adjacent to GaSb and is not detected in the layer above the original interface. The accumulation of Ga and Te at the original interface is probably due to the interaction of Ga and Te with oxygen. However, XRD did not show any peaks related to Ga- O_2 and/or Te- O_2 phases, probably because this region is very thin. A similar SIMS depth profile was obtained for the sample annealed at 100 $^\circ\text{C}$, except the elemental depth profiles did not extend as deep as the layer annealed at 150 $^\circ\text{C}$.

Figures 10(a) and 10(b) show the SIMS depth profiles of the sample annealed at 300 $^\circ\text{C}$ for 30 seconds. In the layer adjacent to the GaSb substrate [Fig. 10(a)], the concentration of Ga increases and Sb decreases, which indicates more Ga (in Au-Ga phases) is accumulated in this layer. The concentration of Ga in the layer above the original interface also increases, which indicates that a large fraction of Ga out-diffuses and reacts with Au. Figure 10(b) shows that C and O_2 remain inert at the original interface even at 300 $^\circ\text{C}$ annealing temperature. This figure also shows that Te concentration in the substrate is about $1 \times 10^{18} \text{ cm}^{-3}$, whereas in the layers on GaSb substrate is about $2\text{-}3 \times 10^{16} \text{ cm}^{-3}$, except at the original interface. The SIMS depth profile

of the sample that was annealed at 400 °C for 30 seconds shows no distinguishable steps within the depth profile as illustrated in Figure 11(a). This is also consistent with the CSSEM micrograph (Figure 2(d)). As shown in Figure 11(b), carbon and oxygen are also distributed throughout the reacted layer, and no sharp interfaces are observed.

E. Electrical Characteristics

The specific contact resistance (SCR) of 0.5- μm -thick Au/GaSb contacts as a function of annealing temperature is shown in Figure 12. The SCR of the p-type samples is independent of the annealing temperature, while the SCR of n-type samples varies with temperature, which indicates that the mechanism for ohmic formation in these two contacts is different. The electrical characteristics of Au/n-type GaSb contacts have diode-like behavior at annealing temperature below 250 °C. The lowest SCR ($6\text{-}7 \times 10^{-6} \Omega\text{-cm}^2$) was obtained when the samples were annealed in the 300-350 °C range for 30 seconds. Beyond this temperature range, the SCR increased. Note, that the SCR of the Au/n-type GaSb when annealed at 300-350 °C range is about 5 times lower than the SCR of Au/p-type GaSb contacts. This result indicates that a thin Au film provides a suitable ohmic contact to n-type GaSb in the 300-350 °C annealing temperature range for 30 seconds. The stability of the SCR of the 0.5- μm -thick Au/n-type GaSb samples were studied by heat treating the samples at 250 °C in an atmospheric ambient after they were annealed at 300 °C for 30 seconds in the RTA system. The SCR's of the samples remain relatively unchanged after heat treatment for 10-30 hours. A summary of the phase transformations and SCR's of the Au/GaSb samples is presented in Table 1.

IV. DISCUSSION AND CONCLUSIONS

Chemical reaction between Au and GaSb occurs at lower annealing temperatures (100 °C) in comparison to Au reactions with other III-V semiconductors such as GaAs, InP or GaP, which occur at over 300 °C. This significant difference in reaction temperature indicates that the reaction mechanism of Au with GaSb is different from other III-V semiconductors. For example, in the Au-GaAs system, GaAs dissolves readily into Au resulting in As and Ga atoms diffusing through the Au film. Arsenic atoms diffuse to the surface and evaporate, while Ga atoms remain in the gold film³⁴. In

contrast, in Au-GaSb system, Au reacts with Sb at the Au-GaSb interface. The low temperature (<100 °C) reaction of Au with GaSb may partially be related to the low bonding energy of Ga-Sb (0.43 eV). This compares with a bonding energy of 1.04 eV for Ga-As. XRD results show that the AuSb₂ compound is partially ordered with respect to the substrate. Based on these observations, we postulate that the Au-GaSb reaction cause replacement of Ga-Sb bonds with Au-Sb bonds at the Au/GaSb interface. Apparently, an activation energy of 0.82 eV is sufficient for this replacement [Fig. 1]. This type of replacement was previously postulated for Co-Hg_{1-x}Cd_xTe³⁵ and Cr-Hg_{1-x}Cd_xTe³⁶. Note that the crystalline structure of AuSb₂ and GaSb are cubic and zincblende, respectively with a lattice mismatch of about 9%. The similarity in crystalline structure of AuSb₂ and GaSb may also facilitate the Au-Ga replacement.

When Au-Sb reacts at the Au/GaSb interface, released Ga atoms enter into the Au film and form Au-Ga alloys and/or compounds. The XRD and SIMS measurements indicate the formation of several phases and phase transitions in Au-Ga system at various annealing temperatures. During the evaporation of Au on Ga, Simic and Marinkovic³⁷ observed the disappearance of the gold color and the interaction of Au and Ga films at room temperature. They reported that the stoichiometry of the resulting compound depends on both the time length and the ratio of Au and Ga concentration. In the Au-GaSb system examined here, a change of gold color at room temperature was not noticed in the time frame of our observation (over a year). However, at higher annealing temperatures a change in surface color and stoichiometry of the resulting Au-Ga component was observed. The difference between the Au-Ga and Au-GaSb cases is that in the Au-GaSb system, Ga atoms need to be released from the Sb bonds in GaSb in order to produce free Ga atoms. This is achieved by the chemical reaction of Au and Sb during the annealing process. As the annealing temperature increases, a larger amount of Ga atoms diffuse to the Au film and various phase transitions occur from lower to higher Au concentration. At a 400 °C annealing temperature, in addition to the surface roughness, dark spots on the surface were observed. The source of these spots could be due to the melt and re-crystallization of Au-Ga, since this temperature is larger than the eutectic temperature (375 °C) of the Au-Ga system.

We have demonstrated that O_2 and C present on the GaSb surface before evaporation remain inert at annealing temperatures below $350^\circ C$, while Au and Ga atoms in-diffuse and out-diffuse across the original interface, respectively. Holloway et al.³⁸ showed that the preparation and etching of GaAs surface is important in the formation of pits. In Au-GaSb system we postulate that the surface condition may not exhibit an important role on the interface reaction because O_2 and C remain at the original Au-GaSb interface. However, we have observed that if the surface of GaSb substrate is not properly cleaned and etched prior to metallization, poor adhesion of as-deposited Au contacts occurs which causes difficulties during the metal lift-off process.

AuGe alloy and AuZn alloy are often used for ohmic contact to n-type or p-type III-V compound semiconductors, respectively. It is well established that during the annealing process, Ge or Zn is incorporated into the surface region as a n^+ -type or p^+ -type dopant by diffusion and/or solidification from a liquid phase. The heavily doped surface regions allow formation of ohmic contacts by the tunneling transport of carriers. In addition to the Au-GaSb contacts investigated in detail in this work, initial electrical measurements were also performed on AuGe-GaSb contacts. When the AuGe alloy was used for ohmic contact to n-type GaSb, the contact resistivity was comparable to unalloyed Au metallization. However, the surface color was darker than normally observed in an unalloyed Au contact (with the same annealing temperature). It is speculated that during the annealing process, Au reacts rapidly with GaSb and leaves Ge behind on the surface of the contact. Since the specific contact resistivity is not changed significantly by the presence of Ge, we suggest that Ge may not have a significant role on the interface reaction and electrical behavior of AuGe-GaSb system. During the sputter deposition of Au and Au-Zn contacts on p-type GaSb, Galzerani, et al.³¹ have shown that the contact resistivity is independent of the presence of Zn in the Au film and the annealing process. They have observed that Zn appear at and near the surface of the contact with annealing. Their results support our hypothesis concerning the role of Ge in AuGe/n-type GaSb contacts.

We have shown that ohmic contacts are formed when unalloyed films of gold are deposited on n-type (Te doped) GaSb and annealed at temperature above $250^\circ C$. Similar behavior was observed with Au contacts to Si-doped GaAs³⁹⁻⁴¹. Holloway et al.³⁸

showed that the transition from Schottky-to-ohmic contact behavior in Au/GaAs contacts is due to the segregation of Si at the original Au-GaAs interface. These heavily n^+ -type doped surface regions allow formation of ohmic contacts by tunneling transport of carriers. However, there are significant differences between the doping behavior in GaSb and most of the other III-V compound semiconductors. Group IV elements are generally n-type dopants in GaAs or InP-based materials and are p-type dopants in GaSb⁴²⁻⁴³. The p-type behavior of group IV elements in GaSb is partly related to the tetrahedral radius of Ga and Sb, since the tetrahedral radius of Sb (1.36 Å) is larger than Ga (1.26 Å), group IV elements preferentially occupy the Sb site. Therefore, the n-type dopants in GaSb are limited to group VI elements, mainly Te. In addition, the highest n-type carrier concentration that can be achieved in GaSb⁴⁴ is about $2-3 \times 10^{18} \text{ cm}^{-3}$, whereas n-type carrier concentration up to mid 10^{19} cm^{-3} range is obtained in GaAs. Therefore, the mechanisms underlying ohmic formation in Au/GaAs contacts can not be utilized for Au/GaSb contacts.

As demonstrated in our SIMS measurements, the Te concentration does not increase at the semiconductor surface during the annealing process. Therefore, we suggest that the transition from Schottky-to-ohmic contact behavior is not dependent on the segregation of n^+ dopants at the Au-GaSb interface. Brilson⁴⁵ presented an alternative model that relates the transition from Schottky-to-ohmic contact behavior to chemical reactions at the metal-semiconductor interface. This model is also not compatible with the transition from Schottky to ohmic behavior in Au-GaSb system, since the chemical reaction occurs at about 100 °C while transition from Schottky- to ohmic-contact behavior occurs at annealing temperature beyond 250 °C.

We suggest an alternative mechanism for ohmic formation, namely, tunneling assisted conduction, where ohmic characteristics are obtained through a series of tunneling transitions of electrons through defects in the depletion region. Riben and Fench⁴⁶ first observed tunneling current via recombination centers at the interface of n-Ge/p-GaAs. Bindal et al.⁴⁷ showed that in PtSi-nSi, with the presence of Al (Cu) at the interface of the contact, a recombination-assisted tunneling current occurs. Weizer and Fatemi⁴⁸ have shown that with the introduction of Ga into Au contact in the Au-InP system, the contact resistivity is decreased by 2-3 orders of magnitude. In the unalloyed

Au/GaSb contact, it is shown that the transition from Schottky- to ohmic-contact behavior occurs simultaneously with the formation of AuGa compound. We speculate that the nature of this tunneling assisted current is the presence of microstructural AuGa phase embedded in the AuSb₂ compound in the depletion region at the AuSb₂/GaSb interface. In this case electrons are assumed to tunnel through a series of local recombination centers (presumably AuGa) from the semiconductor conduction band to the metallic compound. The consistency between the variation of resistivity of Au/n-type GaSb contact and the relative intensity of AuGa x-ray diffraction peaks support this argument.

In the Au/p-type GaSb system, the contacts are ohmic, regardless of the annealing temperature. Furthermore, the contact resistivity is also independent of the annealing temperature in agreement with the others^(15,31). This suggests that the mechanism for ohmic formation in Au/p-type GaSb contact with doping concentration in low-mid 10^{17} cm⁻³ is thermionic emission. This is because the barrier height to the carriers flow between Au and p-type GaSb is negligible and easily overcome by carriers thermal energy. Other metals have also shown ohmic behavior with p-type GaSb¹⁵, regardless of metal work function and annealing temperature. As we have demonstrated, the contact resistivity in Au/n-type GaSb is lower than the contact resistivity of Au/p-type GaSb at comparable doping levels and a certain annealing temperature range. The reason is that the effective mass of electron ($0.041m_0$) in GaSb is smaller than the holes effective mass ($0.4m_0$) by an order of magnitude. Therefore the tunneling assisted mechanism in p-type GaSb contact is insignificant.

V. SUMMARY

The reaction of Au with GaSb occurs at a relatively low temperature (100 °C). Upon annealing, a AuSb₂ compound and several Au-Ga phases are produced. Phase transitions occur toward higher Ga concentration with increasing annealing temperatures. Furthermore, the depth of the contact also increases with increased annealing temperature. We found that the AuSb₂ compound forms on the GaSb surface, with the compound crystal partially ordered with respect to the substrate. The transition of Schottky- to ohmic-contact behavior in Au/n-type GaSb occurs simultaneously with the

formation of the AuGa compound at about a 250 °C annealing temperature. This ohmic contact forms without the segregation of dopants at the metallic compound/GaSb interface. Therefore it is postulated that transition from Schottky- to ohmic-contact behavior is obtained through a series of tunneling transitions of electrons through defects in the depletion region in the Au/n-type GaSb contacts. Contact resistivities of $6-7 \times 10^{-6} \Omega\text{-cm}^2$ were obtained with the annealing temperature between 300 and 350 °C for 30 seconds. In Au/p-type GaSb contacts, the resistivity was independent of the annealing temperature. This suggested that the carrier transport in p-type contact dominated by thermionic emission.

ACKNOWLEDGMENTS

The authors are grateful to Roger Bolen for the cross-sectional SEM measurements and John Barthel for technical assistance.

Table 1. Summary of XRD observations and electrical behaviors for various annealing temperatures and times of 0.5 μm Au evaporated on n-type GaSb substrates.

Annealing Temp. ($^{\circ}\text{C}$)	Annealing time (sec)	Compounds and alloys	Resistivity $\Omega\text{-cm}^2$	Morphology
As-deposited	-----	-----	Schottky diode	Smooth
100	6500	AuSb_2 , $\text{Au}_7\text{Ga}_{2+x}$	Schottky diode	Smooth
150	300	AuSb_2 , Au_2Ga $\text{Au}_7\text{Ga}_{2+x}$	Schottky diode	Smooth
250	30	AuSb_2 , AuGa Au_2Ga , $\text{Au}_7\text{Ga}_{2+x}$	Ohmic 1.2×10^{-5}	Smooth
300	30	AuSb_2 , AuGa Au_2Ga	Ohmic 6.4×10^{-6}	Slightly rough
350	30	AuSb_2 , AuGa Au_2Ga	Ohmic 8.5×10^{-6}	Slightly rough
400	30	AuSb_2 , AuGa_2 AuGa , Au_2Ga	Ohmic 4.2×10^{-5}	Rough (dark spots)

LIST OF FIGURES

FIG. 1. The time required for the disappearance of gold color as a function of the reciprocal of the annealing temperature for a 0.5- μm -thick Au film deposited on a (001) GaSb substrate.

FIG. 2. Cross-sectional scanning electron images of a 0.5- μm -thick Au film deposited on a (001) GaSb substrate annealed (a) as-deposited, (b) at 150 °C for 300 seconds, (c) at 300 °C for 30 seconds, and (d) at 400 °C for 30 seconds.

FIG. 3. XRD spectra of as-deposited 0.5- μm -thick Au film on a (001) GaSb substrate. The x-ray diffraction peaks correspond to polycrystalline Au and single crystal GaSb.

FIG. 4. XRD spectra of a 0.5- μm -thick Au film on a (001) GaSb substrate, annealed at 100 °C for 1.8 hours. The x-ray diffraction peaks correspond to single-crystal GaSb, AuSb₂ and Au₇Ga_{2+x}.

FIG. 5. XRD spectra of a 0.5- μm -thick Au film on a (001) GaSb substrate, annealed at 150 °C for 5 minutes. The x-ray diffraction peaks correspond to single-crystal GaSb, AuSb₂, Au₂Ga, and Au₇Ga_{2+x}.

FIG. 6. XRD spectra of a 0.5- μm -thick Au film on a (001) GaSb substrate, annealed at 250 °C for 30 seconds. The x-ray diffraction peaks correspond to single-crystal GaSb, AuSb₂, AuGa, Au₂Ga, and Au₇Ga_{2+x}.

FIG. 7. XRD spectra of a 0.5- μm -thick Au film on a (001) GaSb substrate, annealed at 300 °C for 30 seconds. The x-ray diffraction peaks correspond to single-crystal GaSb, AuSb₂, AuGa, and Au₂Ga.

FIG. 8. XRD spectra of a 0.5- μm -thick Au film on a (001) GaSb substrate, annealed at 400 °C for 30 seconds. The x-ray diffraction peaks correspond to single-crystal GaSb, AuSb₂, AuGa₂, AuGa, and Au₂Ga.

FIG. 9. SIMS depth profile of a 0.5- μm -thick Au film on a (001) GaSb substrate and annealed at 150 °C for 300 seconds. (a) Secondary ion intensity of Au, Sb, and Ga. (b) concentration of Te (n-type dopant in substrate), O₂, and C.

FIG. 10. SIMS depth profile of a 0.5- μm -thick Au film on a (001) GaSb substrate and annealed at 300 °C for 30 seconds. (a) Secondary ion intensity of Au, Sb, and Ga. (b) concentration of Te (n-type dopant in substrate), O₂, and C.

FIG. 11. SIMS depth profile of a 0.5- μm -thick Au film on a (001) GaSb substrate and annealed at 400 °C for 30 seconds. (a) Secondary ion intensity of Au, Sb, and Ga. (b) concentration of Te (n-type dopant in substrate), O₂, and C.

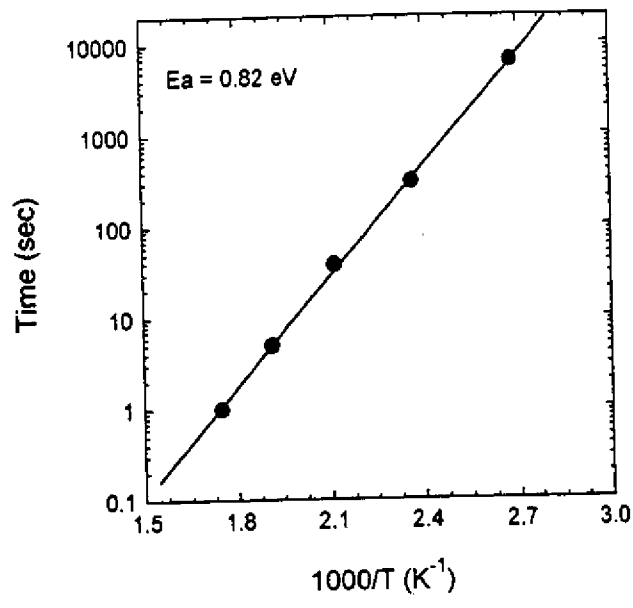
FIG. 12. Contact resistivity as a function of annealing temperature for 0.5- μm -thick Au deposited on n-type (Te doped) and p-type (undoped) (001) GaSb substrates.

REFERENCES

- ¹M. O. Manasreh, Ed. Antimonide-Related Strained-Layer Heterostructures, Optoelectronic Properties of Semiconductors and Superlattices, Vol 3. (Gorden Breanch Scientific Publishers, Amsterdam, 1997).
- ²A. G. Milnes and A. Y. Polyakov, *Solid-State Electronics*, Vol. 36, 803 (1993).
- ³P. S. Dutta, H. L. Bhat, and V. Kumar, *J. Appl. Phys.* **81**, 5821 (1997).
- ⁴G. W. Charache, P. F. Baldasaro, L. R. Danielson, M. D. DePoy, M. J. Freeman, C. A. Wang, H. K. Choi, D. Z. Garbuzov, R. U. Martinelli, V. Khalfin, S. Saroop, J. M. Borrego, and R. J. Gutmann, *J. Appl. Phys.* **85**, 2247 (1999).
- ⁵Fourth NREL Conference on Thermophotovoltaic Generation of Electricity [AIP Conf. Proc. (1998)].
- ⁶K. Taira, F. Nakamura, I. Hase, and Y. More, *J. Cryst. Growth* **107**, 952 (1991).
- ⁷S. R. Kurtz, L. R. Dawson, T. E. Zipperian, and S. R. Lee, *Appl. Phys. Lett.* **52**, 1581 (1988).
- ⁸M. J. Howe and D. V. Morgan, *Gallium Arsenide Materials, Devices and Circuits*, Wiley, New York (1985).
- ⁹T. J. Kim and P. H. Holloway, *Critical Review in Solid-State and Materials Sciences*, **22**, 239 (1997).
- ¹⁰N. S. Fatemi and V. G. Weizer, *J. Appl. Phys.* **73**, 289 (1991).
- ¹¹I. Lindau, P. W. Chye, C. M. Garner, P. Pianetta, C. Y. Su, and W. E. Spicer, *J. Vac.*
- ¹²P. W. Chye, I. Lindau, P. Pianetta, C. M. Garner, and W. E. Spicer, *Phys. Rev. B* **17**, 2682 (1978).
- ¹³F. A. Kroger, G. Dimer, H.A. Klasens, *Phys. Rev.* **103**, 279 (1956).
- ¹⁴W. E. Spicer, I. Lindau, P. Skeath, C. Y. Su, and Patrick Chye, *Phys. Rev. Lett.* **44**, 420 (1979).
- ¹⁵A. G. Milnes, M. Ye, and M. Stam, *Solid-State Electron.* **37**, 37 (1994).
- ¹⁶J. B. B. Oliveira, C. A. Oliviera, J. C. Galzerani, A. A. Pasa, and F. C. de Prince, *J. Appl. Phys.* **66**, 5484 (1989).
- ¹⁷A. Subekti, V. W. L. Chin, and T. L. Tansley, *Solid-State Electron.* **39**, 329 (1996).
- ¹⁸W. S. Tse, R. H. Chen, C. S. Ares Fang, and J. R. Chen, *Appl. Phys. A* **54**, 556 (1992).

- ¹⁹P. H. Holloway, L. Lu-Min Yeh, D. H. Powell, and A. Brown, *Appl. Phys.* **59**, 947 (1991).
- ²⁰T. Kendelewicz, W. G. Petro, I. Lindau, and W.E. Spicer, *J. Vac. Sci. Technol.* **B2**, 453 (1994).
- ²¹N. S. Fatemi and V. G. Weizer, *J. Appl. Phys.* **67**, 1934 (1990).
- ²²E. Villemain, S. Gaillard, M. Rolland, and A. Jollie, *Mater. Sci. Eng. B* **20**, 162 (1993).
- ²³Y. K. Su, N. Y. Li, F. S. Juang and S. C. Wu, *J. Appl. Phys.* **68**, 646 (1990).
- ²⁴C. H. Heinz, *Int. J. Electronics*, **54**, 247 (1983).
- ²⁵A. Subekti, V. W. L. Chin, and T. L. Tansley, *Solid-State Electronics*, **39**, 329 (1996).
- ²⁶B. Tadayon, C. S. Kyono, M. Fatemi, S. Tadayon, and J. A. Mittereder, *J. Vac. Sci. Technol.* **B13**, 1 (1995).
- ²⁷E. Villemain, S. Gaillard, M. Rolland, and A. Joullie, *Materials Science and Engineering*, **B20**, 162 (1993).
- ²⁸X. Li and A. G. Milnes, *J. Electrochem. Soc.* **143**, 1014 (1996).
- ²⁹S. S. Tan and A. G. Milnes, *Materials Science and Engineering*, **B21**, 94 (1993).
- ³⁰W. S. Tse, R. H. Chen, C. S. Ares Fang, and J. R. Chen, *Appl. Phys.* **A54**, 556 (1992).
- ³¹J. C. Galzerani, A. M. Oyama, P. S. Pizani, R. Landers, S. L. Morelhao, and L. P. Cardoso, *Materials Science and Engineering*, **B20**, 328 (1993).
- ³²R. H. Cox and H. Strack, *Solid-State Electron.* **10**, 1213 (1967).
- ³³B. Pecz, R. Veresgyhazy, A. Barna, I. Mojzes, and G. radnoczi, *Proceeding of the 17th AVS/IUVSTA International Conference on Thin Films/Metallurgical Coatings*, San Diego, 1990.
- ³⁴I. Mojzes, T. Sebestyen, and D. Szegethy, *Solid-State Electron.* **25**, 449 (1982).
- ³⁵H. Ehsani and R. W. Bene, *J. Appl. Phys.* **63**, 1478 (1998).
- ³⁶J. P. Haring, J.G. Werthen, and R. H. Bube, *J. Vac. Sci. Technol. A* **1**, 1469 (1983).
- ³⁷V. Simic and Z. Marinkovic, *Thin Solid Films*, **34**, 179 (1976).
- ³⁸P. H. Holloway and C. H. Mueller, *Thin Solid Films*, **221**, 254 (1992).
- ³⁹A. K. Sinha, and J.M. Poate, *Appl. Phys. Lett.* **23**, 666 (1973).
- ⁴⁰Liu L. M. Yeh, Y.J. Xie, C. Mueller, and P. H. Holloway, *J. Vac. Sci. Technol. A*, 1532 (1987).
- ⁴¹C. L. Bauer, *Surf. Sci.* **168**, 395 (1986)

- ⁴²H. Ehsani, I. Bhat, R. Gutmann, and G. Charache, *Appl. Phys. Lett.* **69**, 3863 (1996).
- ⁴³K. F. Longenbach, S. Xin, and W. I. Wang, *J. Appl. Phys.* **69**, 3393 (1991).
- ⁴⁴H. Ehsani, I. Bhat, C. Hitchcock, R. J. Gutmann, G. Charache, and M. Freeman, *J. Crys. Growth*, **195**, 385 (1998).
- ⁴⁵L. J. Brillson, *J. Vac. Sci. Technol.* **15**, 1378 (1978).
- ⁴⁶A. R. Riben and D. L. Feucht, *Solid State Electron*, **9**, 1055 (1966).
- ⁴⁷A. Bindal, R. Wachnik, and W. Ma, *J. Appl. Phys.*, **68**, 6259 (1990).
- ⁴⁸V. G. Weizer and N. S. Fatemi, *J. Appl. Phys.* **69**, 8253 (1991).



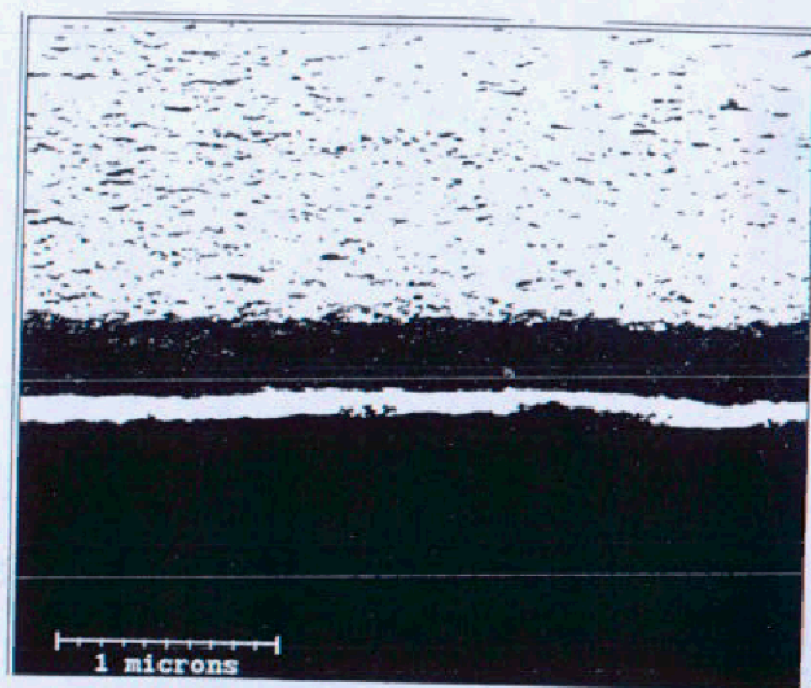


Fig. 2(a)

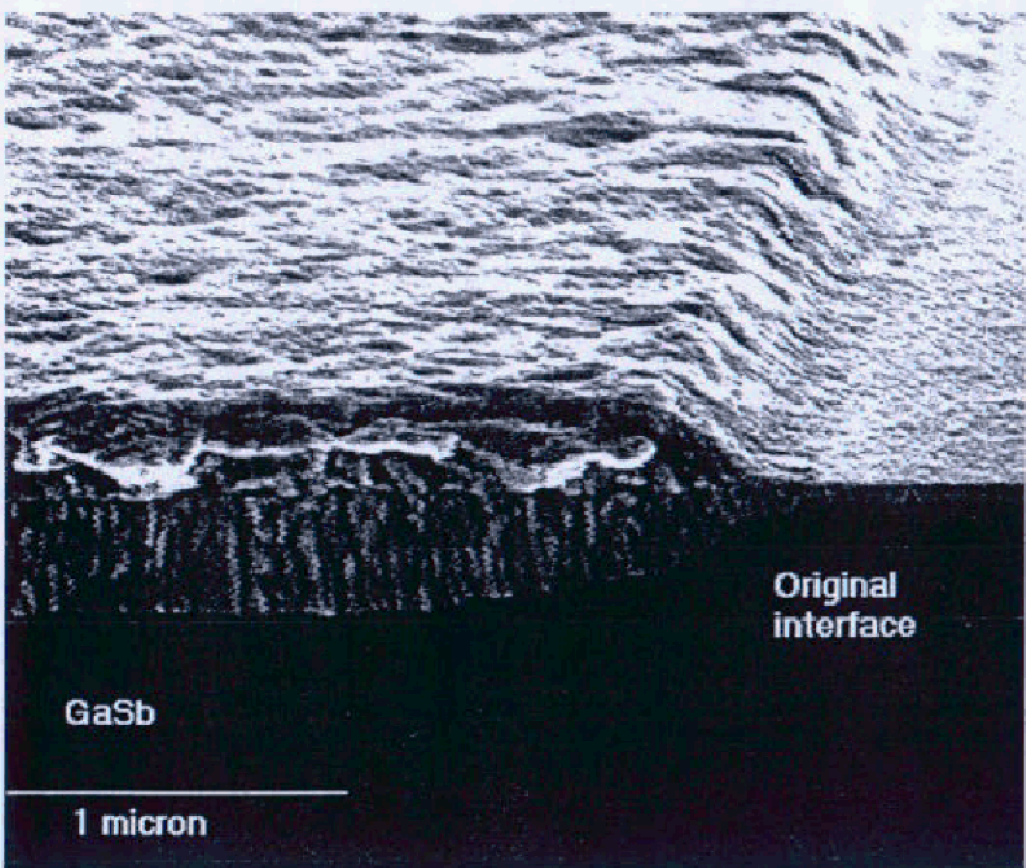


Fig 2(b)

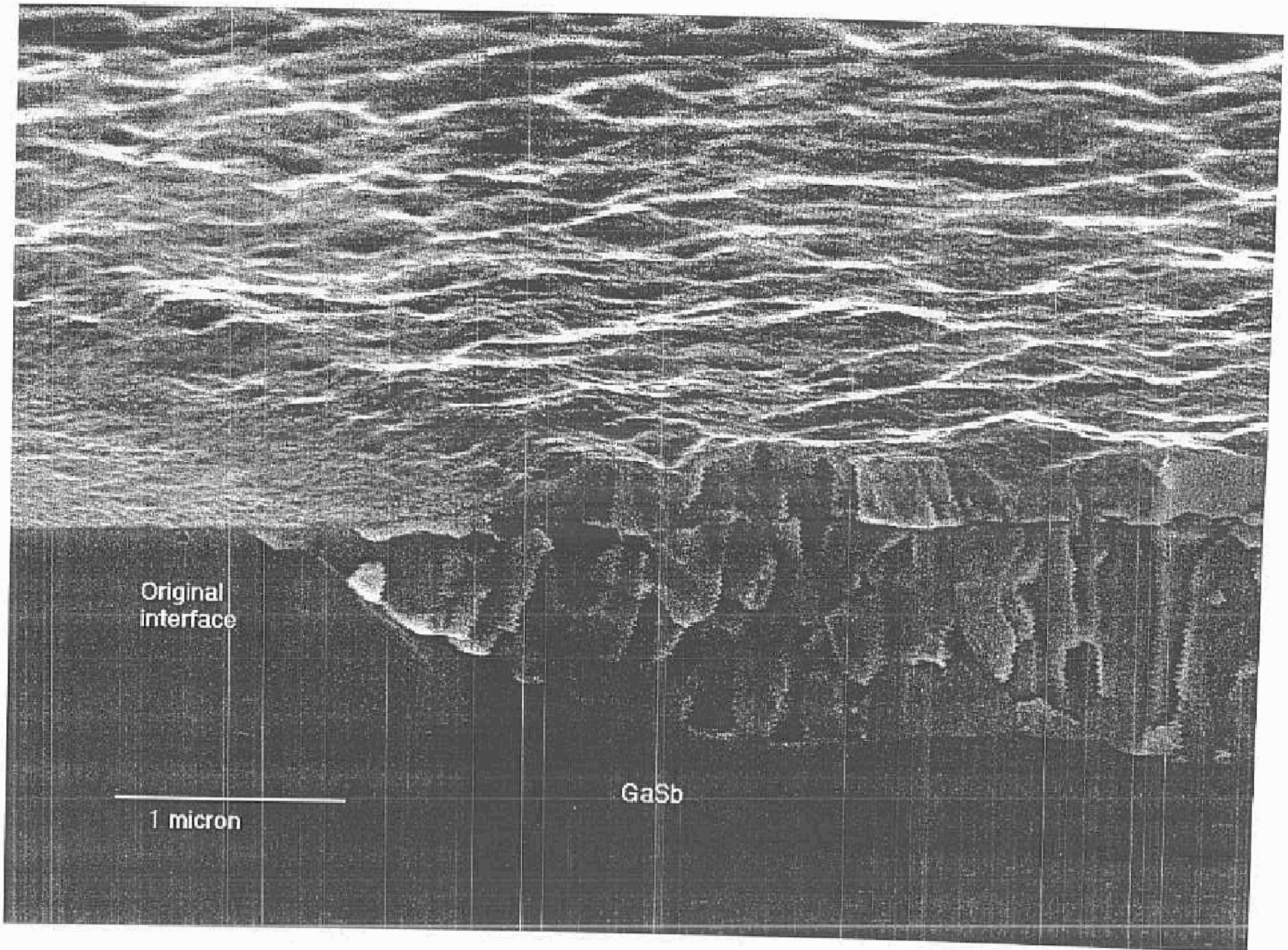


Fig 2(c)

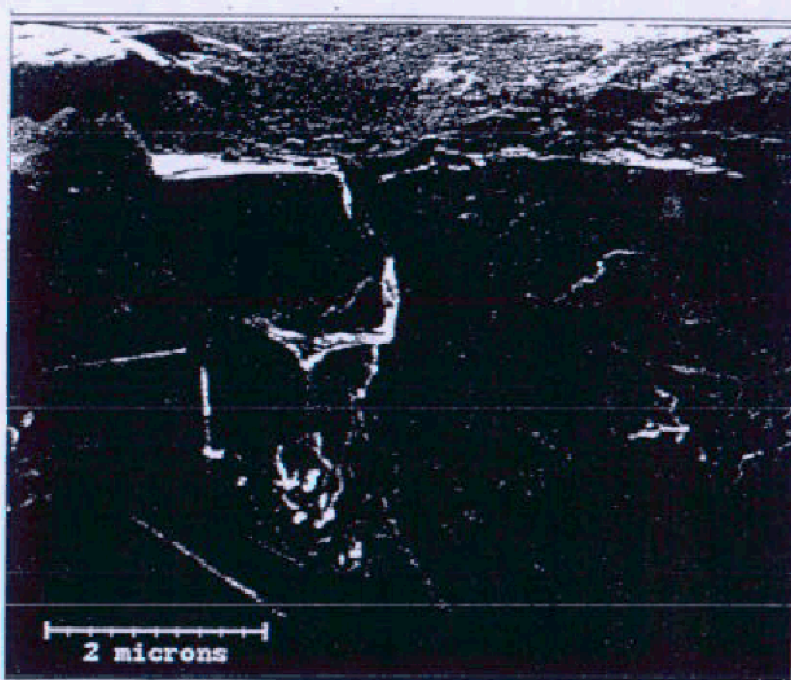


Fig. 2(d)

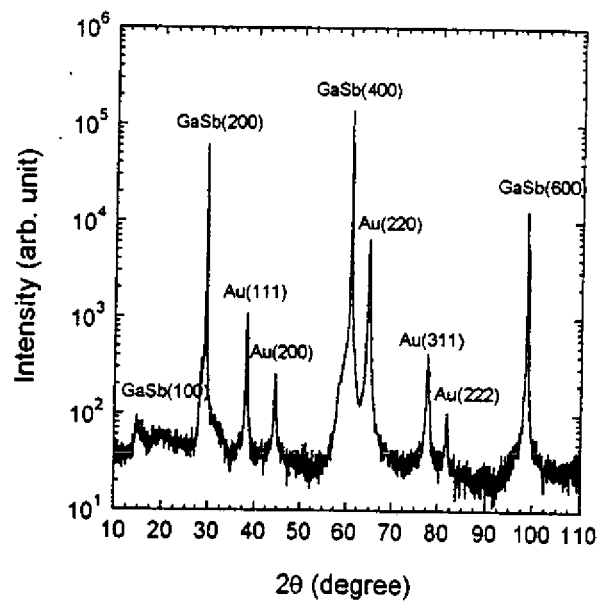


Fig. 3

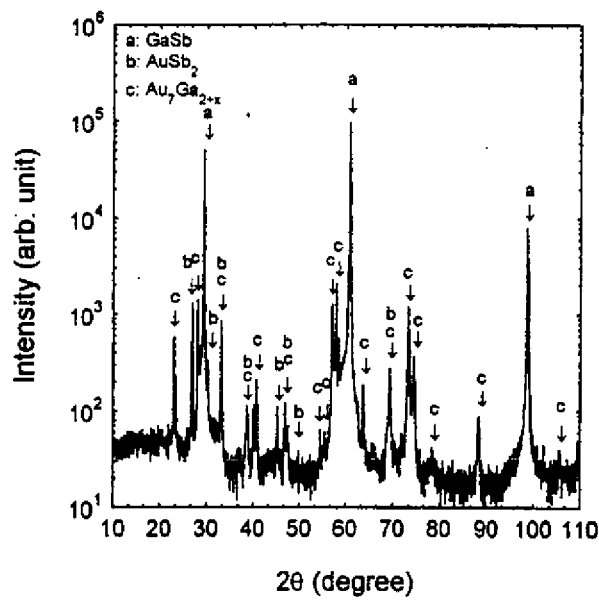
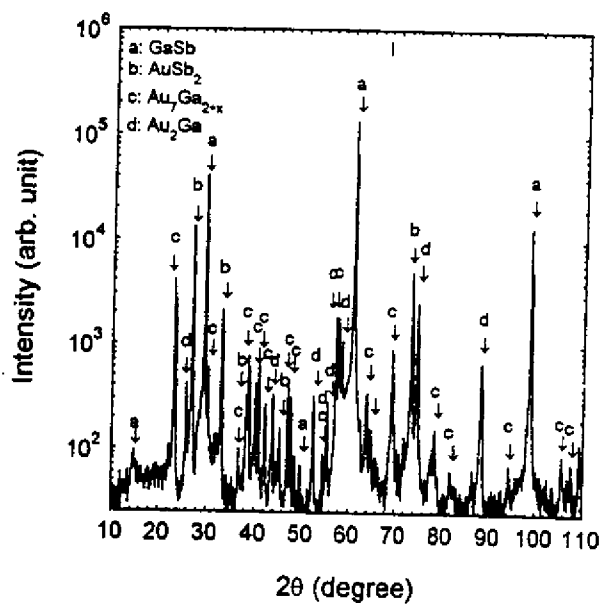


Fig 4



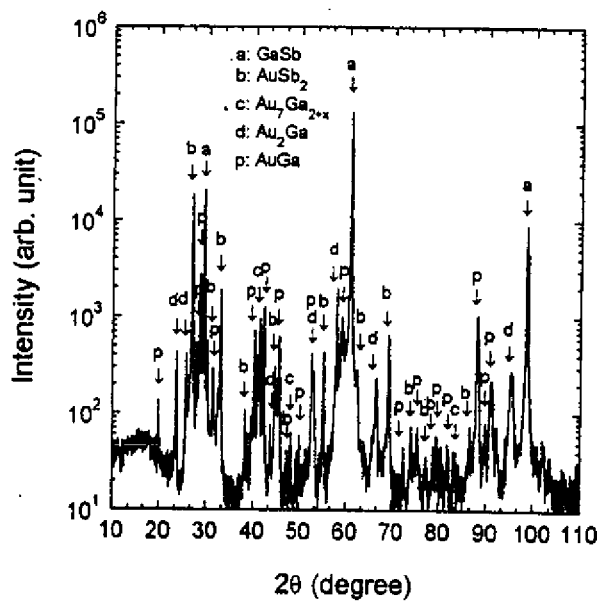


Fig 6

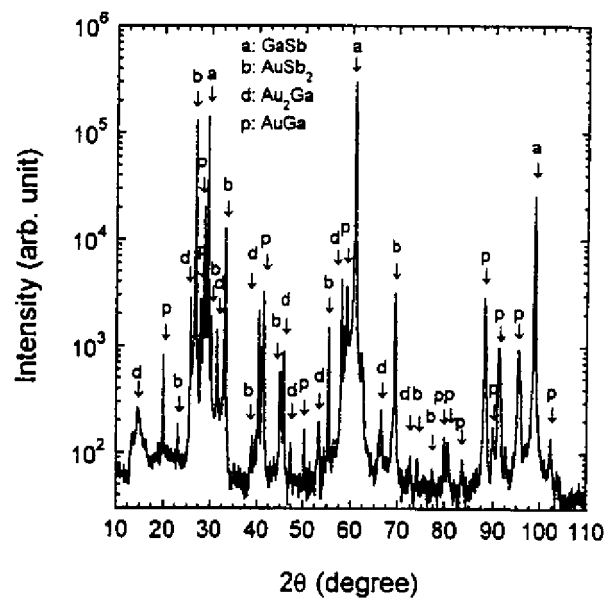


Fig 7

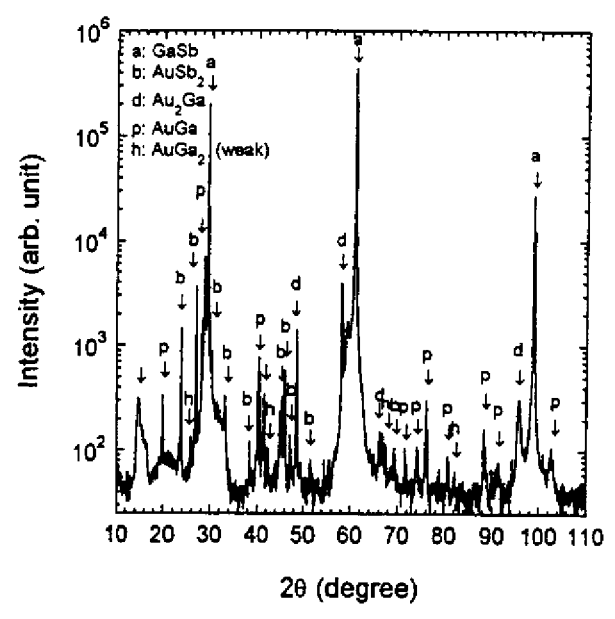


Fig. 8

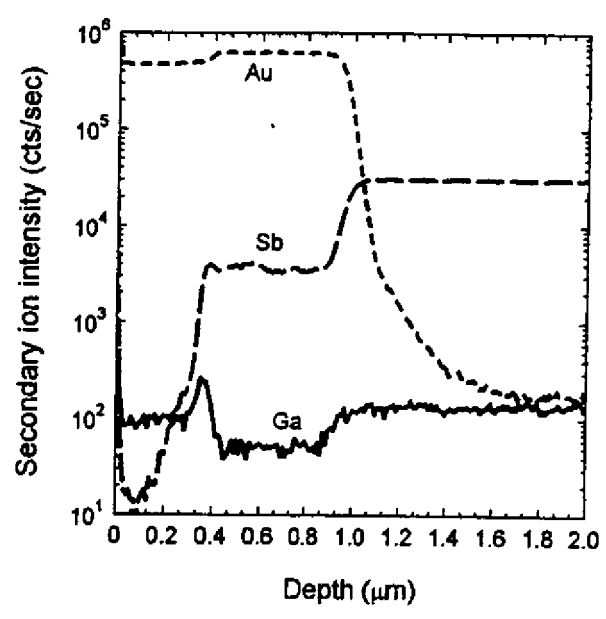


Fig 9(a)

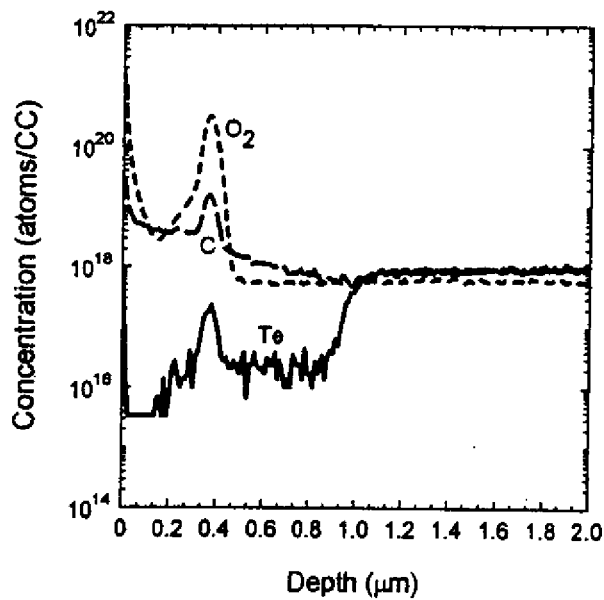


Fig 9(b)

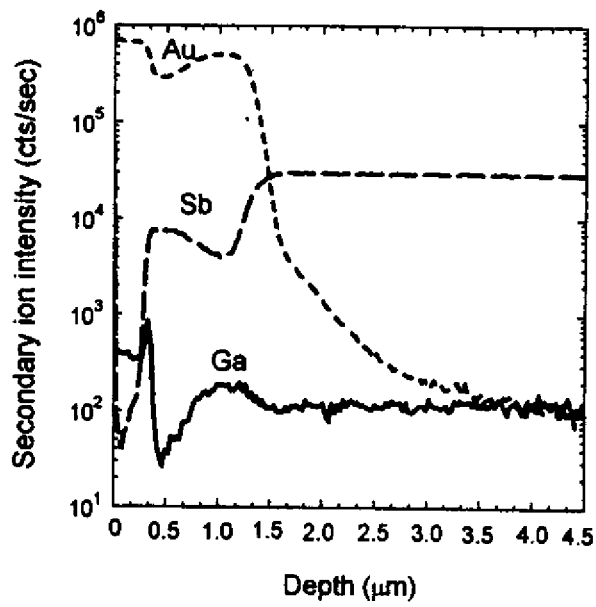


Fig 10(a)

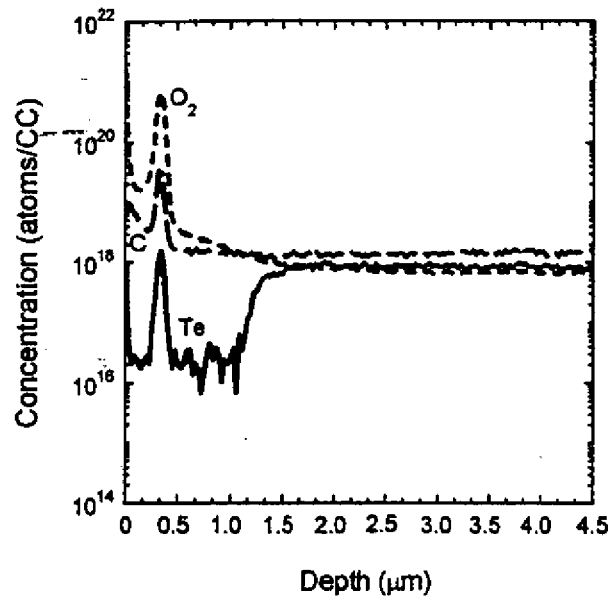


Fig 10(b)

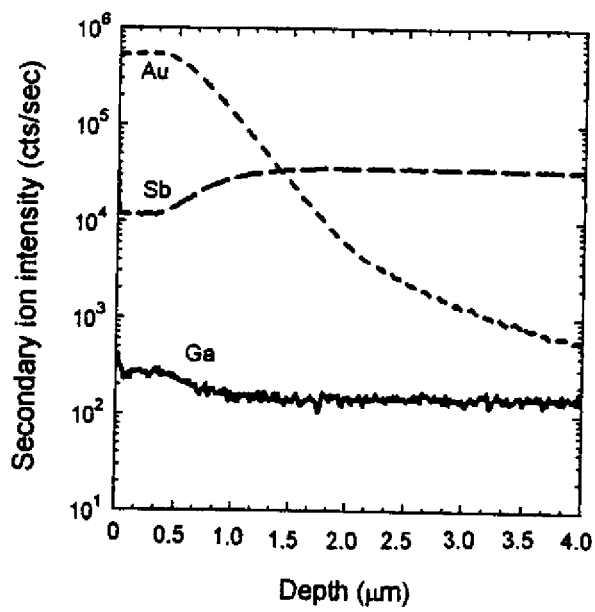


Fig. 11(a)

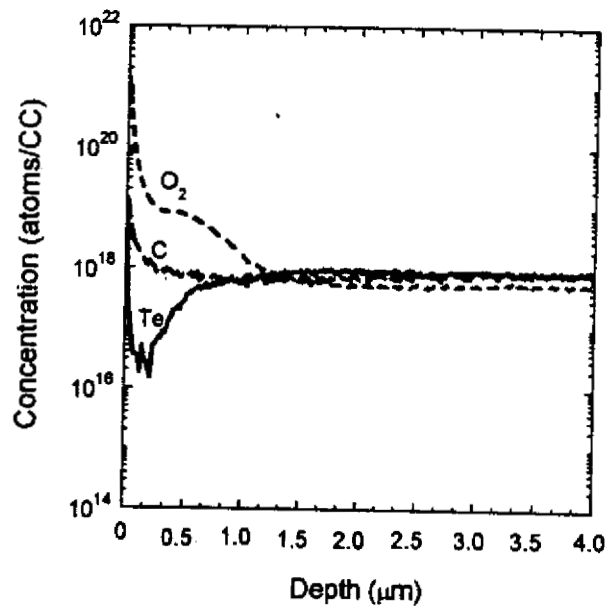


Fig. 11(b)

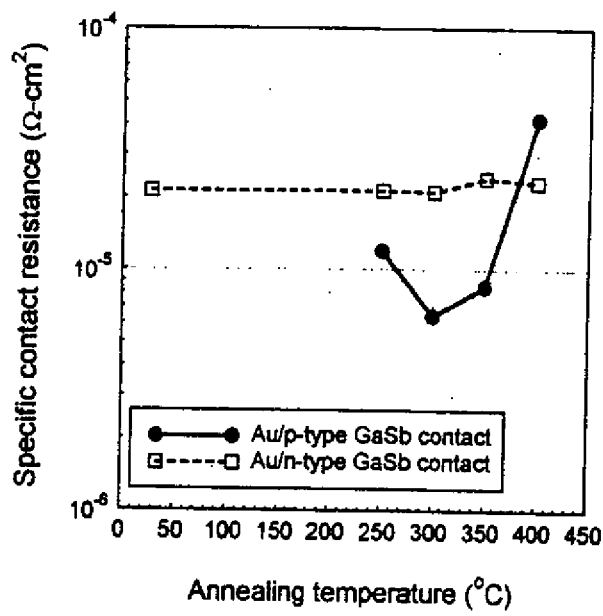


Fig. 12